Communications

Microscopic Mechanism of Specific Peptide Adhesion to Semiconductor Substrates[**]

Michael Bachmann, Karsten Goede,* Annette G. Beck-Sickinger, Marius Grundmann, Anders Irbäck, and Wolfhard Janke

In the past few years, the interest in hybrid interfaces formed by soft molecular matter and hard solid substrates has rapidly grown as such systems promise to be relatively easily accessible candidates for novel biosensors or electronic devices. The enormous progress in high-resolution microscopy and in biochemical engineering of macromolecules is the major prerequisite for studies of hybrid systems and potential applications.[1,2] One particularly important problem is the self-assembly and adhesion of polymers, proteins, or protein-like synthetic peptides to solid materials, such as metals,[3,4] semiconductors,[5–8] carbon and carbon nanotubes,[9,10] and silica.[11,12] Peptide and substrate specific binding affinity is particularly relevant in pattern-recognition processes.[13,14] Systematic experimental studies have been performed to investigate binding properties of individual amino acids in their binding behavior to selected materials.[15] Basic theoretical considerations of simplified polymer–substrate and protein–substrate models have predicted complex pseudo-phase diagrams.[16,17]

In bacteriophage display experiments, only a few peptides out of a library of 10^9 investigated sequences with 12 amino acid residues were found to possess a particularly strong propensity to adhere to GaAs(100) surfaces.[5] The sequence specificity of adsorption strength is a remarkable property, but the question remains as to how it is related to the individual molecular structure of the peptides. We expect that relevant mutations of sites in the amino acid sequence can cause a change of the binding affinity. Indeed, one key aspect of our study is to show that proline is a potential candidate for switching the adsorption propensities to cleaned Si(100) substrates.

Silicon is one of the technologically most important semiconductors, as it serves, for example, as carrier substrate in microelectronics. For this reason, electronic and surface properties of silicon have been thoroughly investigated, such as oxidation processes in air[18,19] and water[20,21] as well as the formation of hydride surface structures and the silicon-binding characteristics of small organic compounds.[6,22]

To guide the design of peptide–silicon interfaces, we first performed extensive computer simulations of a novel hybrid model (see below). To test the theoretically revealed trends of adsorption propensity changes by selected mutation, we synthesized the suggested specific mutants by means of multiple solid-phase peptide synthesis. The theoretical predictions were subsequently verified in atomic force microscopy (AFM) experiments (see Figure 1 and the detailed descriptions in the Supporting Information).

The hybrid model used in the computer simulations is composed of two parts contributing to the energy $E(X)$ of a peptide conformation X: the energy of the peptide as represented by an implicit-solvent all-atom model[23,24] and the interaction of the peptide with the substrate, which is modeled in a simplified way. The peptide model takes into account intrinsic excluded volume repulsions between all atoms, a local potential that represents the interaction among neighboring NH and CO partial charges, hydrogen bonding energy, and the interaction between hydrophobic side chains.[23,24] The substrate model consists only of atomic layers with surface specific atomic density and planar surface structure. In this simplified model, each peptide atom feels the mean field of the atomic substrate layers. The atomic density of these layers depends on the crystal orientation of the substrate at the surface. Based on these assumptions, a generic noncovalent Lennard-Jones approach for modeling the interaction between peptide atoms and surface layer is

[*] Dr. M. Bachmann
Institut für Festkörperforschung, Theorie II
Forschungszentrum Jülich (Germany)

Dr. K. Goede, Prof. M. Grundmann
Institut für Experimentelle Physik II
Universität Leipzig
Linnéstrasse 5, 04103 Leipzig (Germany)
Fax: (+49) 341-9732668
E-mail: goede@physik.uni-leipzig.de

Prof. A. G. Beck-Sickinger
Institut für Biochemie, Universität Leipzig (Germany)

Dr. M. Bachmann, Prof. A. Irbäck
Computational Biology & Biological Physics
Department of Astronomy and Theoretical Physics
Lund University (Sweden)

Dr. M. Bachmann, Prof. W. Janke
Institut für Theoretische Physik, Universität Leipzig (Germany)

Supporting information for this article, including the precise modeling of the hybrid system, the multicanonical simulation methodology, and details of the peptide selection, the AFM experiments, and the sample preparation, is available on the WWW under http://dx.doi.org/10.1002/anie.201000984.
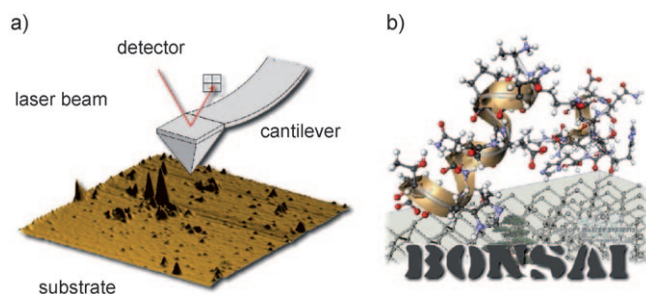
Figure 1. a) Principle of the atomic force microscope. The original AFM image exhibits S1 peptide clusters on an oxidized $10\times10\,\mu m^2$ silicon substrate. The height of the highest cluster is 56 nm. b) Computer simulations were performed with the BONSAI package that we developed for Monte Carlo simulations of peptide models. The snapshot shows S1 peptides forming helical segments near a silicon substrate. (BONSAI = bioorganic nucleation and self-assembly at interfaces.)

employed.[9,25] We have studied this model by means of multicanonical computer simulations,[26] which provide us with canonical statistics for any temperature T. The partition function is thus given by $Z = \int DX\, e^{-E(X)/RT}$, where DX is the formal functional integral measure for all possible conformations X in the space of the degrees of freedom. The statistical average of any quantity O is $\langle O\rangle = Z^{-1}\int DX\, O(X)\, e^{-E(X)/RT}$. In our simulations, the integral is estimated by an average over a large set of conformations (in each run about 10^9 updates were performed) selected by multicanonical importance sampling. The precise modeling of the hybrid system and the multicanonical simulation methodology are described in the Supporting Information.

The peptide with the amino acid sequence S1 (Figure 2a) is a good example for the substrate specificity of adsorption. In recent comparative adsorption experiments, it could be shown that although S1 binds strongly to GaAs(100), binding to Si(100) is very weak.[7,8] In contrast, the adhesion is strongly increased, if the Si substrate is oxidized. This can clearly be seen in Figure 2a, where AFM images of S1 adhered at a deoxidized (left) and an oxidized Si(100) substrate (right) are shown. Peptide covered regions appear bright. A quantitative measure for the binding propensity is the peptide adhesion coefficient (PAC), which is the relative area of the surface covered by peptide clusters.[7,8] These PAC values are determined by means of a cluster analysis of the respective AFM images. To reduce the dependence on the peptide concentration in solution, we introduce the calibrated PAC (cPAC) as the ratio of PACs measured for the binding of the peptides to Si(100) and GaAs(100) substrates under identical conditions. GaAs(100) is chosen as a reference substrate, as the peptides considered herein bind comparatively well to this substrate. The cPAC charts for S1 in Figure 2b clearly indicate the difference of binding affinity at cleaned and oxidized substrates.

This result is different for sequence S3 (for sequence and AFM images, see Figure 2c), which is a random permutation of S1 with unchanged amino acid content. Surprisingly, the binding propensity of S3 to Si(100) was found to be much larger than that of S1.[8] In this case, the binding affinities at cleaned and oxidized Si(100) substrates are similarly strong,
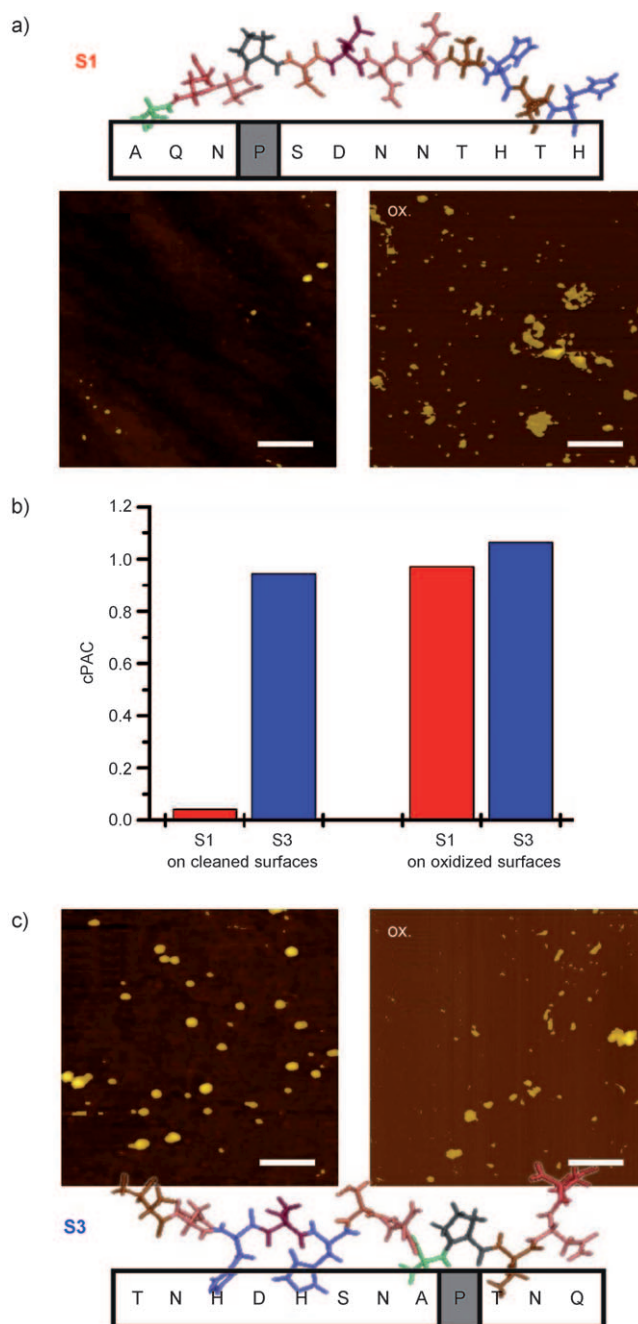
Figure 2. Adsorption to cleaned and oxidized substrates. AFM images of peptides a) S1 and c) S3 adsorbed to cleaned (deoxidized) and oxidized Si(100) surfaces. The AFM scale bar is 1 μm. b) Calibrated peptide adhesion coefficients (cPAC) for S1 and S3 adsorption to cleaned and oxidized Si(100) substrates. Amino acids occurring in the peptides of our study are alanine (A), aspartic acid (D), histidine (H), asparagine (N), proline (P), glutamine (Q), serine (S), and threonine (T).

as the cPAC charts for S3 in Figure 2b show. In recent computational analyses of the solvent properties of these peptides, we have shown that also the folding behaviors in solution exhibit noticeable differences.[27] This is also true at room temperature, where in both cases the population of the structurally different native folds is rather small.

Another remarkable result of this former computational study is that the qualitative folding behaviors of S1 and S3 are related to each other if these sequences are mutated pairwise at the position of proline, which occurs once in the sequences S1 and S3.[27] The mutated sequence S1′ differs from S1 only by the exchange of proline at position 4 and threonine at 9 (Figure 3a). Similarly, in S3′, proline at 9 is exchanged with
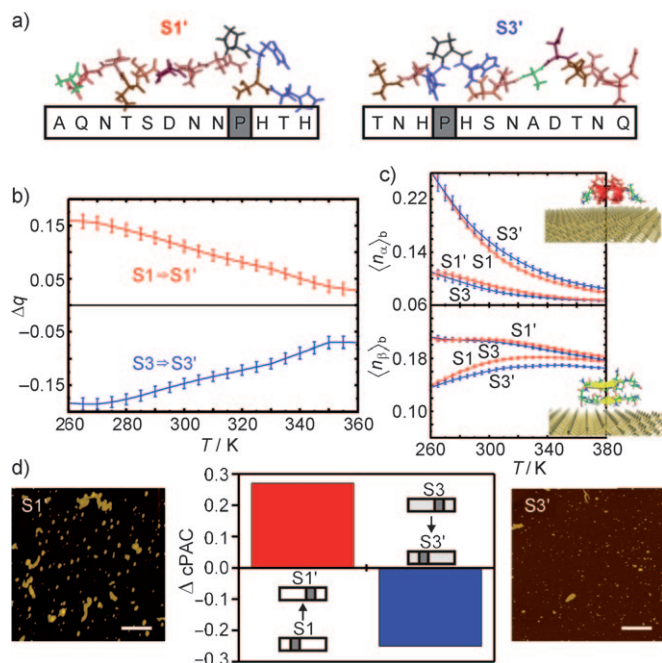
Figure 3. Reversed adsorption propensity of proline-mutated peptides (see text for details). a) Proline-mutated sequences S1′ and S3′. b) Adsorption parameter Δq, as a function of temperature, from our computer simulations. c) α-Helix content $\langle n_\alpha \rangle_b$ and β-strand content $\langle n_\beta \rangle_b$ of bound peptides. Conformations depicted in the insets are lowest-energy structures identified in the simulations (with rather small populations at room temperature) and represent the preferred trends in secondary-structure formation. d) Confirmation by AFM experiments at room temperature. AFM scale bars: 1 μm.

the aspartic acid at 4, compared to S3 (Figure 3a). These replacements were rationalized by the presumption that the particular steric properties of proline, and thus its place in the sequence, influence the folding. It turned out that the folding behavior of S1′ in solution is indeed close to that of S3, whereas S3′ behaves rather like S1.[27] Before we can address the question as to whether these results are also of relevance for the adsorption behavior to Si(100), we need to discuss microscopic properties of deoxidized Si(100) substrates.

In our experiments, the Si(100) surfaces were first cleaned in a solution of ammonium fluoride (NH₄F) and hydrofluoric acid (HF).[7,8] The peptide adsorption process then took place in deionized water. This standard procedure ensures that the silicon surface is virtually free of oxide and possesses strongly hydrophobic properties[18,20] (for sample preparation and experimental details, see the Supporting Information). The initial Si−F bonds after etching are replaced by Si−H bonds in the rinsing process in deionized water. After drying the sample, AFM scans of the surface were performed. Although

the oxidation also proceeds in water,[20,21] there are clear indications (maximum water droplet contact angle after removing the samples off the peptide solution) that the hydrophobicity of the silicon samples remains largely intact during the peptide adsorption process. It is also known that silicon surfaces are comparatively rough after HF treatment.[22] Thus, the reactivity of the surface is influenced by steps, which depend on the offcut and its directions. This renders an atomistic modeling intricate, and even more so as Si(100) 2 × 1 surfaces are also known to form Si−Si dimers on top of the surface[6] with highly reactive dangling bonds. From the considerations and the experimental preparations described above, it seems plausible that these bonds are mainly passivated by hydrogen, forming hydride layers.[6,20,22] It should be emphasized that under these conditions, the surface structure of Si(100) is substantially different from oxidized Si(100), which is polar and in effect hydrophilic.[18] An important result of Figure 2 is that the binding of S1 and S3 to oxidized GaAs(100) and Si(100) surfaces is virtually independent of the substrate type (cPAC ≈ 1). Thus, the top oxygen layer screens the substrate from the peptide. The different adhesion propensities to the clean (hydrated) substrates (see also Figure 2) lead to the conclusion that oxidation has not yet strongly progressed during the peptide adsorption process. We conclude that the key role of water is the slowing down of the oxidation process of the Si(100) surface, but for the actual binding process its influence is rather small. In particular, we do not expect that stable water layers form between adsorbate and substrate.

These characteristic properties of HF-treated Si(100) surfaces in deionized water effectively enter into the definition of our hybrid model of the peptide–silicon interface (for details see the "Model and Methods" section of the Supporting Information), which serves as the basis for our theoretical analysis and interpretation of the specificity of peptide adhesion on these interfaces.

To quantify the degree of adsorption, we define the ratio of heavy (non-hydrogen) atoms located in a distance $z_i \leq 5$ Å from the substrate, n_h, and the total number of heavy atoms, N_h, as the adsorption parameter $q = n_h/N_h$. The temperature dependence of its relative change by proline mutation, $\Delta q(Sn \rightarrow Sn') = (\langle q(Sn') \rangle - \langle q(Sn) \rangle)/\langle q(Sn) \rangle$ (with $n = 1,3$), is shown in Figure 3b. The main result is that due to this selective mutation, the Si(100) adsorption affinity from S1 to S1′ increases ($\Delta q(S1 \rightarrow S1') \approx +0.11$ at $T = 300$ K), whereas it decreases by about the same amount as S3 is mutated to S3′ ($\Delta q(S3 \rightarrow S3') \approx -0.15$ at $T = 300$ K).

This result is directly connected with the tendency to form secondary structures. In Figure 3c, the respective α-helix content (ratio of the dihedral Ramachandran angles of the inner 10 residues satisfying $\phi \in (-90°, -30°)$ and $\psi \in (-77°, -17°)$) and β-strand content (dihedral angles in the intervals $\phi \in (-150°, -90°)$ and $\psi \in (+90°, +150°)$) of the bound peptides are shown. We define a peptide in a certain conformation as bound to the substrate if at least 2% of the heavy atoms are within a 5 Å distance from the surface. There is a clear tendency that residues of S1 and S3′ are rather in an α state and residues of S3 and S1′ are in a β state. However, the small secondary-structure contents are quite similar to

what we found for the peptides in solution (without substrate),[27] which were qualitatively consistent with analyses of CD spectra.[8] It is a noticeable result that secondary structures herein are not stabilized near the cleaned Si(100) substrate, whereas in recent adsorption experiments of a synthetic peptide binding at silica nanoparticles, a stabilization of α helices was observed.[12]

The experimental results shown in Figure 3d compared to those in Figure 2a and c confirm that the proline mutation of S1 indeed increases the Si(100) binding affinity, whereas an analogous mutation decreases the binding strength of S3 by about the same value: the substrate coverage for S1′ increases and that of S3′ decreases. By measuring the associated cPAC values, we find that $\Delta\text{cPAC}(\text{S1}\rightarrow\text{S1}') = \text{cPAC}(\text{S1}')-\text{cPAC}(\text{S1}) \approx +0.27$ and $\Delta\text{cPAC}(\text{S3}\rightarrow\text{S3}') \approx -0.25$. This convincingly confirms our theoretical prediction from the hybrid-model simulations.

In summary, we have predicted by computer simulations and verified by AFM experiments that a selected proline mutation of short peptides facing a deoxidized silicon substrate can substantially change the binding affinity in a very predictive and specific way. We could also show that this behavior is in part due to a qualitatively different folding behavior of the mutated sequences in the vicinity of the substrate. The proline position most likely also affects the aggregation properties[8] of the peptides and thereby indirectly again their binding characteristics. Building up on simulations of single-molecule behavior, such as those discussed in the present manuscript, simulating coupled folding and aggregation while binding will therefore constitute a rewarding future project. Gaining deeper insights into the general principles of binding specificities is a first fundamental step towards the design of nanosensors with specific biomedical applications. Thus, the extension of our study to biomolecules is natural and the identification of unique bioprotein adsorption signals in experiments with nanoarrays of several materials is a prerequisite for future applicability of such hybrid systems in biotechnology.

[1] M. Sarikaya, C. Tamerler, A. K.-Y. Jen, K. Schulten, F. Baneyx, *Nat. Mater.* **2003**, *2*, 577–585.
[2] J. J. Gray, *Curr. Opin. Struct. Biol.* **2004**, *14*, 110–115.
[3] S. Brown, *Nat. Biotechnol.* **1997**, *15*, 269–272.
[4] L. Delle Site, C. F. Abrams, A. Alavi, K. Kremer, *Phys. Rev. Lett.* **2002**, *89*, 156103.
[5] S. R. Whaley, D. S. English, E. L. Hu, P. F. Barbara, A. M. Belcher, *Nature* **2000**, *405*, 665–668.
[6] J. M. Buriak, *Chem. Rev.* **2002**, *102*, 1271–1308.
[7] K. Goede, P. Busch, M. Grundmann, *Nano Lett.* **2004**, *4*, 2115–2120.
[8] K. Goede, M. Grundmann, K. Holland-Nell, A. G. Beck-Sickinger, *Langmuir* **2006**, *22*, 8104–8108.
[9] R. Hentschke, *Macromol. Theory Simul.* **1997**, *6*, 287–316.
[10] S. Wang, E. S. Humphreys, S.-Y. Chung, D. F. Delduco, S. R. Lustig, H. Wang, K. N. Parker, N. W. Rizzo, S. Subramoney, Y.-M. Chiang, A. Jagota, *Nat. Mater.* **2003**, *2*, 196–200.
[11] H. Heinz, H. Koerner, K. L. Anderson, R. A. Vaia, B. L. Farmer, *Chem. Mater.* **2005**, *17*, 5658–5669.
[12] M. Lundqvist, P. Nygren, B.-H. Jonsson, K. Broo, *Angew. Chem.* **2006**, *118*, 8349–8353; *Angew. Chem. Int. Ed.* **2006**, *45*, 8169–8173.
[13] A. J. Golumbfskie, V. S. Pande, A. K. Chakraborty, *Proc. Natl. Acad. Sci. USA* **1999**, *96*, 11707–11712.
[14] T. Bogner, A. Degenhard, F. Schmid, *Phys. Rev. Lett.* **2004**, *93*, 268108.
[15] R. L. Willett, K. W. Baldwin, K. W. West, L. N. Pfeiffer, *Proc. Natl. Acad. Sci. USA* **2005**, *102*, 7817–7822.
[16] M. Bachmann, W. Janke, *Phys. Rev. Lett.* **2005**, *95*, 058102.
[17] M. Bachmann, W. Janke, *Phys. Rev. E* **2006**, *73*, 020901(R).
[18] R. G. Frieser, *J. Electrochem. Soc.* **1974**, *121*, 669–672.
[19] A. Hemeryck, N. Richard, A. Estève, M. Djafari Rouhani, *Surf. Sci.* **2007**, *601*, 2339–2343.
[20] L. Ling, S. Kuwabara, T. Abe, F. Shimura, *J. Appl. Phys.* **1993**, *73*, 3018–3022.
[21] M. K. Weldon, B. B. Stefanov, K. Raghavachari, Y. J. Chabal, *Phys. Rev. Lett.* **1997**, *79*, 2851–2854.
[22] Y. J. Chabal, K. Raghavachari, *Phys. Rev. Lett.* **1984**, *53*, 282–285.
[23] A. Irbäck, S. Mohanty, *Biophys. J.* **2005**, *88*, 1560–1569.
[24] A. Irbäck, S. Mohanty, *J. Comput. Chem.* **2006**, *27*, 1548–1555.
[25] W. A. Steele, *Surf. Sci.* **1973**, *36*, 317–352.
[26] B. A. Berg, T. Neuhaus, *Phys. Rev. Lett.* **1992**, *68*, 9–12.
[27] S. Mitternacht, S. Schnabel, M. Bachmann, W. Janke, A. Irbäck, *J. Phys. Chem. B* **2007**, *111*, 4355–4360.